High open-circuit voltage Mos2 homojunction - effect of Schottky barriers at the contacts

Bueno Blanco, Carlos; Svatek, Simon Aurel; Lin, Der-Yuh; Macias Evangelista, Carlos; García Sánchez, Marcos; Zehender, Marius Harry; Watanabe, Kenji; Taniguchi, Takashi; García-Linares Fontes, Pablo and Antolín Fernández, Elisa

▶ To cite this version:

C. Bueno-Blanco *et al*., "High open-circuit voltage Mos2 homojunction - effect of Schottky barriers at the contacts," *2020 47th IEEE Photovoltaic Specialists Conference (PVSC)*, Calgary, AB, Canada, 2020, pp. 0324-0329, doi: 10.1109/PVSC45281.2020.9301009.

Published Version.

Published 2021 January 05

High open-circuit voltage MoS_2 homojunction - effect of Schottky barriers at the contacts

Carlos Bueno-Blanco
Universidad Politécnica de Madrid
Instituto de Energía Solar
Madrid, Spain.
carlos.buenob@upm.es

Simon A. Svatek
Universidad Politécnica de Madrid
Instituto de Energía Solar
Madrid, Spain.
simon.svatek@upm.es
ORCID: 0000-0002-8104-1888

Der-Yuh Lin
Department of Electronics Engineering
National Changua University of Education.
Changua, Taiwan.
dylin@cc.ncue.edu.tw

Carlos Macías
Universidad Politécnica de Madrid
Instituto de Energía Solar
Madrid, Spain.
c.macias@alumnos.upm.es

Marcos García-Sánchez
Universidad Politécnica de Madrid
Instituto de Energía Solar
Madrid, Spain.
marcos.gsanchez@alumnos.upm.es

Marius H. Zehender
Universidad Politécnica de Madrid
Instituto de Energía Solar
Madrid, Spain
marius.zehender@upm.es

Kenji Watanabe
Advanced Materials Laboratory
National Institute for Materials Science
Tsukuba, Japan
watabe.kenji.aml@nims.go.jp

Takashi Taniguchi
International Center for Materials
Nanoarchitectonics
National Institute for Materials Science
Tsukuba, Japan
taniguchi-takashi@nims.go.jp

Pablo García-Linares
Universidad Politécnica de Madrid. Solar
Instituto de Energía Solar
Madrid, Spain.
p.garcia-linares@upm.es

Elisa Antolín
Universidad Politécnica de Madrid
Instituto de Energía Solar
Madrid, Spain.
elisa.antolin@upm.es
ORCID: 0000-0002-5220-2849

***Abstract*— Van der Waals structures made of layered semiconductor materials, such as transition metal dichalcogenides (TMDCs), have been proposed for the development of ultra-thin photovoltaic devices. The main limitation of these solar cells up to now has been their low open-circuit voltage (V_{OC}), which is typically below 0.55 V even for high illumination levels. Recently, we have presented a *p-n* MoS_2 homojunction that exhibits a V_{OC} of 1.02 V under broadband illumination equivalent to 20 suns. The use of substitutionally-doped *p* and *n* MoS_2 material instead of a heterojunction is crucial to produce a band alignment that enables high V_{OC}. Another important aspect for the realization of large photovoltages in TMDC solar cells is the optimization of metallic contacts. We demonstrate using a simple circuital model that the presence of Schottky barriers at the semiconductor/metal interfaces does not only introduce a non-ohmic series resistance, but also reduces the V_{OC} because the Schottky diodes are photoactive. We characterize the Schottky barrier produced by different metals in combination with *p* and *n* MoS_2. When *p*-flakes are deposited directly onto a SiO_2/Si substrate, we find that they are depleted from carriers by a surface doping effect. This depletion contributes to aggravate the effect of the *p*-MoS_2/metal Schottky. We show that inserting a flake of hexagonal boron nitride (h-BN) between the *p*-material and the SiO_2 surface eliminates this effect. Given the already demonstrated strong light absorption of TMDC ultra-thin devices, the achievement of high V_{OC} is a turning point in the path towards high-efficiency TMDC solar cells.**

Keywords*— *2D Materials, layered materials, transition metal dichalcogenides, van der Waals structures, Schottky barrier, homojunctions, ultra-thin solar cells.

I. INTRODUCTION

Layered TMDCs are promising candidates for photovoltaic applications due to their strong light-matter interaction, chemical stability, and ease assemble in ultra-thin structures. TMDC crystals are composed by multiple layers which are weakly bonded to each other through van der Waals forces. These flakes can be exfoliated, and electronic devices can be built by stacking them on top of each other. The absence of dangling bonds at the surfaces makes it possible to assemble ultra-thin devices without the impact of a high surface recombination velocity.

Ultra-thin solar cells based on van der Waals structures have been developed in previous works, mostly based on heterojunctions of MoS_2 and WSe_2 [1-3]. Although these devices show strikingly high photocurrent for their thicknesses, none of them provided V_{OC} values over 0.55 V, which is a low threshold compared to the materials band gap energies (1.2 and

1.9 eV for MoS_2 in bulk form and monolayer [4], respectively; 1.2 and 1.7 eV in the case of WSe_2).

MoS_2 is probably the most studied layered TMDC. It is naturally an *n*-type semiconductor, presumably due to a high concentration of native sulfur vacancies. However, recent studies have developed a procedure to produce stable *p*-type MoS_2 using niobium as substitutional dopant [5]. This has opened the path to produce stable vertical MoS_2 *p-n* homojunctions based on van der Waals assembly [6]. In our recent work [7] we show that using *n* and *p* doped MoS_2 it is possible to achieve V_{OC} values higher than reported for heterojunctions, demonstrating for the first time V_{OC} = 1 V in a van der Waals solar cell without the addition of an external electric field (gating). Here, we study the impact of the Schottky barriers formed at the TMDC/metal interfaces on the photovoltage produced by homojunction TMDC solar cells.

II. HIGH VOLTAGE P-N JUNCTION

Fig 1.a shows the structure of a *p-n* MoS_2 van der Waals homojunction. *N*-type MoS_2 is doped with Fe and *p*-type is doped with Nb. The nominal concentration of substitutional dopant atoms is 0.5% in both cases. Details on the material properties are given elsewhere [5].

The flakes (~ 10 nm) were exfoliated and transferred onto a SiO_2/Si substrate using the hot pick-up technique [8]. Four electrical contacts were defined using mask-less photolithography, and metals (15 nm Ni and 85 nm Au) were deposited by physical vapor deposition (PVD).

Fig 1.b shows the 4-wire current density-voltage (*J-V*) curves when the device is illuminated with a halogen lamp (irradiance 2 W/cm^2, equivalent to approximately 20 AM1.5G suns). These results have been reported in [7]. It can be observed that a high V_{OC} is reached, 0.73 V, when the whole device is illuminated, and even higher, 1.02 V, when the light is partially blocked so that it impinges only on the *p-n* junction. In this device it is possible to achieve a 1V V_{OC} because it is a MoS_2 homojunction and not a heterojunction. Therefore, the V_{OC} is limited by the built-in voltage and not by the heterojunction offset [7].

We find that the difference in V_{OC} value between the two curves in Fig. 1 can be explained by the effect of photoactive Schottky diodes at the semiconductor-metal contacts. Many studies have reported the formation of rectifying Schottky barriers between TMDC flakes and different metals. Such contacts are expected to degrade the fill factor (FF) of a solar cell, but usually not its V_{OC}. However, we find in the case of TMDC solar cells, the Schottky barriers at the contacts have an impact on both FF and V_{OC}. To understand this behavior, we have developed a numerical model based on the equivalent circuit represented in Fig. 2, where we have included the *p-n* homojunction and two reverse biased Schottky diodes. The model can be used to fit two-wire (Fig. 2a) and four-wire (Fig. 2b) measurements. The Schottky contacts can be numerically modelled as diodes [9]:

$$I = KT^2(1 - exp(\frac{qV}{nk_bT})) \qquad (1)$$

Where K is a constant, q is the electron charge, V the voltage, n the diode ideality factor, k_b the Boltzmann constant and T the temperature, which is 300 K. For the *p-n* homojunction we use the Shockley diode equation.

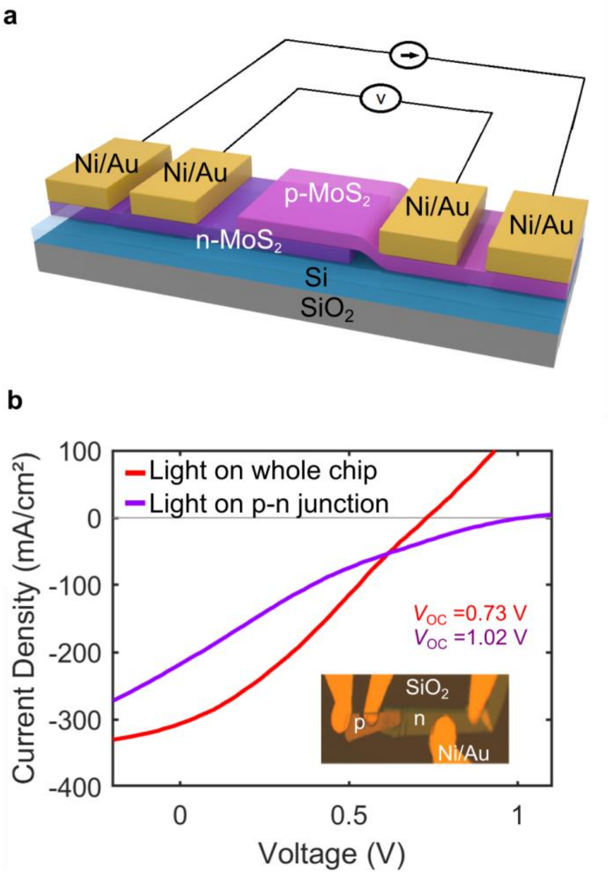

Fig 1. (a) MoS_2 homojunction device structure. (b) Four wire *J-V* curves under halogen lamp spectrum; irradiance level 2 W/cm^2. When the whole chip is illuminated the V_{OC} value is pinned to 0.73V. If only the *p-n*-junction area is illuminated, the V_{OC} reaches 1.02 V. Inset: micro-photograph of the device.

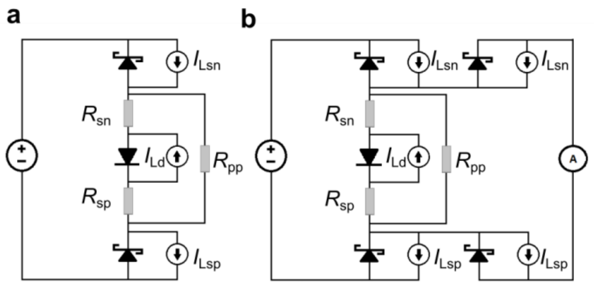

Fig 2. Equivalent electrical circuit for the sample shown in Fig. 1. (a) Two-wire configuration. (b) Four-wire configuration.

This work has been funded by the Spanish Science Ministry under Grant TEC2017-92424-EXP and by Fundación Ramón Areces within the research project SuGaR. C.B-B and M.H.Z. are grateful to Universidad Politécnica de Madrid for funding through the Predoctoral Grant Programme. S.A.S acknowledges a Juan de la Cierva Fellowship (FJC2018-036517-I) and E.A. acknowledges a Ramón y Cajal Fellowship (RYC-2015-18539), both funded by the Spanish Science Ministry.

In the model we assume that the Schottky diodes are photoactive and introduce I_{Lsp} and I_{Lsn} as the illumination currents of the *p*-contact and *n*-contact, respectively. Both are proportional to the *p-n* junction illumination current I_{Ld}. R_{sn} and R_{sp}, are the series resistance of each flake, and R_{pp} the shunt resistance.

We find that the model correctly fits all *J-V* curves recorded for a given device under different illuminations, and with two and four wires. In Fig. 3 we plot the model fitting for the experimental curves in Fig. 1. Panel a corresponds to the case where the whole chip is illuminated and panel b to the case where only the *p-n* junction is illuminated. In both plots, the red dots are the experimental data and the red curve is the fit. We have also plotted the contributions of the different elements in the model: blue represents the *J-V* characteristic of the *p-n* junction alone and golden (green) the *J-V* characteristic of the p-Schottky (n-Schottky).

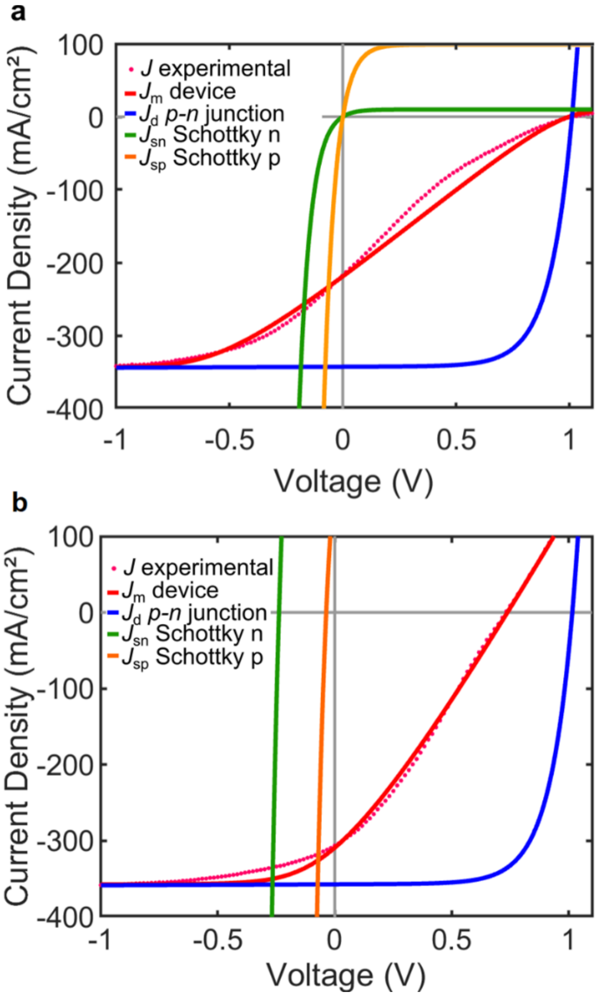

Fig 3. Theoretical modeling of the *J-V* curves shown in Fig 1b. (a)Whole chip illuminated. (b) Ligth on *p-n* junction only.

In Fig. 3a, where the Schottky contacts are not illuminated, the total V_{OC} (red curve) approaches the *p-n* junction V_{OC} of 1.02 V (blue curve). However, in Fig. 3b it can be observed that the photovoltages produced at the metal-semiconductor contacts (0.25 V at the n-Schottky and 0.04 V at the p-Schottky) are reducing the total V_{OC} of the device to 0.73 V. This means that the 1V V_{OC} better illustrates the potential of MoS_2 homojunctions. Also, it means that in practical devices the *J-V* curves are severely affected by the presence of a parasitic reverse-biased diode at each TMDC/metal interface (more detrimental in his case on the n-flake).

It is important to note that the Schottky contacts are photoactive although the metal has been deposited on top of the semiconductor flakes. The metal is thick enough to block the light, but the depletion region of the metal-semiconductor contact expands laterally because the flakes are very thin, and therefore the photoactive region is not limited to the area under metal and has variable size, as it has been shown in [10].

Another important conclusion from the model is that the series resistance of the device depends on the illumination level. This can be attributed to a partial depletion of the TMDC flakes, which get populated with photocarriers under illumination. From the model fitting we obtain that the total series resistance of the device is 1.78 $\Omega\cdot cm^2$ when the whole device is illuminated and 4.18 $\Omega\cdot cm^2$ when only the *p-n* junction is illuminated.

The height of a Schottky barrier is, in a first approximation, a function of the difference between the metal work function and the semiconductor electron affinity. TMDCs have been proven to suffer strong Fermi-level pinning at their surfaces which makes that the actual Schottky barrier differs from the theoretical predictions (except for extremely perfect semiconductor/metal interfaces [11]). However, there is still in most cases a noticeable dependence of the Schottky barrier height on function of the metal [12]. In our case, *p*-MoS_2 makes good electrical contact with nickel, whereas *n*-MoS_2 forms a strong Schottky barrier with that metal.

The effect of the Schottky barriers on the *J-V* curves of the solar cell can be visualized using photocurrent mapping. In this technique, we scan the sample with a micrometric laser spot and record the photocurrent generated by different device areas.

We have mapped the photocurrent of the MoS_2 *p-n* junction shown in Fig. 4a. In this device, the MoS_2 flakes have been deposited on pre-patterned Au contacts on a glass substrate. Fig. 4 b, c and d show photocurrent maps obtained with a 550 nm wavelength laser and spot size 10 μm^2, aplying a bias voltage of 0, 0.1 and 0.2 V, respectively.

In Fig. 4b, it is perceptible that the *p*-MoS_2/metal contact acts as a parasitic diode generating a photocurrent with opposite sign to the current delivered by the *p-n* junction. However, the photocurrent produced by the *p*-contact is low in comparison to that produced by the *p-n* junction. By applying a forward bias to the device, as in Fig. 4c and Fig. 4d, the photocurrent generated by the Schottky contact is enhanced because the parasitic diode is reverse biased. This behavior, which is in complete agreement with our modeling results (Fig. 2 and Fig. 3) explains the observed V_{OC} pinning in TMDC devices and why the pinning is released if the semiconductor/metal contacts are kept in the dark.

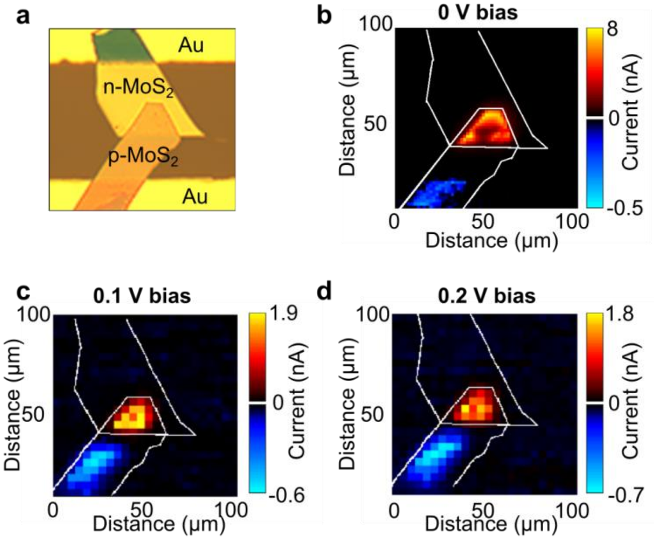

Fig 4. MoS_2 *p-n* junction on Ni/Au contacts. (a) Device. (b) 0 V bias photocurrent map. (c) 0,1 V bias voltage photocurrent map. (d) 0.2 V bias voltage photocurrent map.

In Fig. 4b, when the voltage bias is zero, only the area directly above the metal generates enough photocurrent to be noticed. When the bias is increased in plots c and d, the photoactive area spreads towards the *p-n* junction, which can be related to the growth of the carrier depletion region as the Schottky diode is reverse biased. A similar effect is expected when the metallic contacts lie on top of the semiconductor flakes.

In the case of Fig. 4, the *n*-Schottky could not be visualized in the map due to the low illumination level. We have observed that Schottky contacts which are not noticebable in a photocurrent map can still have a significant impact on the V_{OC} of the TMDC solar cells under moderate illuminations.

III. SCHOTTKY CONTACT CHARACTERIZATION

We have said that in our MoS_2 homojunction solar cell with Ni/Au contacts, the n-Schottky is more detrimental than the p-Schottky. Here, we characterize the Ni/n-MoS_2 Schottky using the sample shown in Fig. 5a. It consists of a flake of *n*-MoS_2 exfoliated onto a SiO_2/Si substrate. Ni/Au contacts have been deposited by photolithography and PVD on top of the flake. These contacts are identical to the ones used in our solar cell.

Fig. 5b shows *J-V* curves in the dark and under illumination with a halogen lamp (irradiance 2W/cm^2). The curves are non-ohmic and very resistive, and the conductivity increases under illumination. The electrical circuit equivalent to these structures consists of two opposite Schottky diodes with their corresponding current generators. Therefore, the dark current is limited by the reverse saturation current of the reverse-biased diode, whereas under illumination the current flow can be larger due to the photogeneration of the Schottky diodes. Note that, again, this photogeneration occurs although the metals are deposited on top of the semiconductor. The photosensitivity cannot be explained by a change in the conductivity of the flake because the illuminated curve exhibits a V_{OC}. Either Schottky barrier is producing a photovoltage and they do not cancel out because the two contacts are not identical.

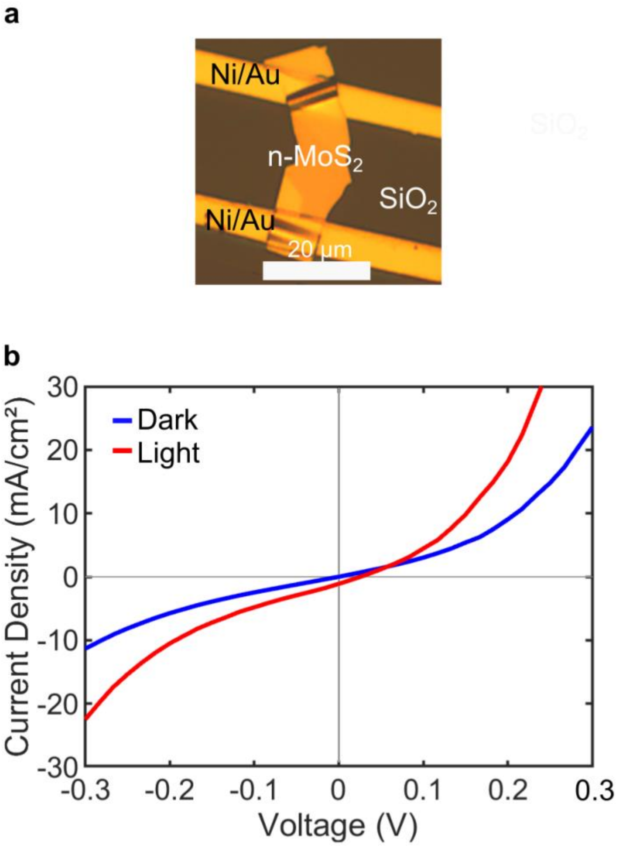

Fig 5. (a) Device (A). (b) *J-V* curves illuminating the whole device, the positive side and negative side.

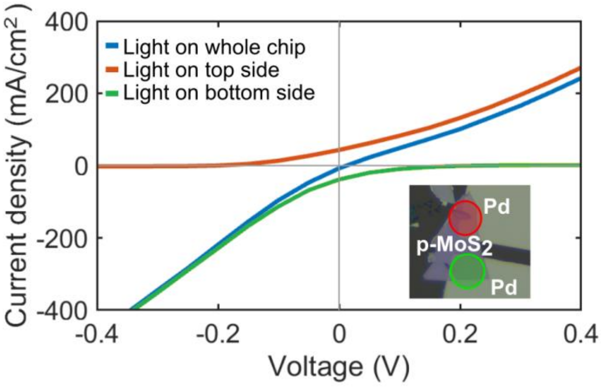

Fig 6. *J-V* curves of p-MoS_2 flake on Pd contacts. Blue curve corresponds to the whole device illuminated; green curve has the light on the positive side and red curve on the negative side. Inset: micro-photograph of the device. The red (green) circle represents the area illuminated to measure the red (green) curve.

Fig. 6 shows another example of Schottky contacts to MoS_2, in this case a *p* doped flake. Here the flake has been deposited onto pre-patterned palladium contacts. Because in this case the metal is under the semiconductor, the effect of the photogeneration at that Schottky diodes is easily identified. It is even possible to illuminate only one contact to see how the photogeneration on that Schottky diode enables the current flow in one direction.

IV. DEPLETION OF P-FLAKE

In ultra-thin devices, such as our TMDC solar cells, the characteristic of the semiconductor/metal contact and therefore, the performance of the solar cell can be influenced by the substrate on which the device is built. Charge concentration supplied by the substrate onto the surface of the material can induce band bend at the surface of the semiconductor flake, and therefore, changes in the carrier population [13]. This effect could in principle aggravate or alleviate the effect of Schottky contacts. We have observed that this surface doping effect is specially detrimental for *p*-MoS_2 flakes deposited onto SiO_2 and it can be eliminated by inserting a flake of hexagonal boron nitride (h-BN) between the *p*-MoS_2 flake and the SiO_2/Si substrate.

In Fig. 7 two devices are shown, both with Pt contacts processed by mask-less photolithography on a SiO_2/Si substrate. On the metal contacts, a *p*-MoS_2 flake has been deposited. In Fig. 7.c, it is plotted the current obtained when a source-drain voltage (V_{sd}) of 0.1 V is applied between the contacts as a function of gate voltage (V_G, voltage applied to the Si substrate).

The device in Fig. 7a suffers a reduction of the conductivity as the gate voltage increases, which implies that the flake is easily depleted. However, when a h-BN flake is placed below the semiconductor, as in the device in Fig. 7.b, the conductivity is constant, as expected from degeneretelly doped *p*-MoS_2. This result is consitent with the observation of superficial n-doping of MoS_2 from SiO_2 substrates reported by other groups [13].This effect can be specially detrimental for TMDC devices if it appears in combination with a Schottky barrier at the metal interface. Therefore, introducing an h-BN buffer under the p-flake is important for the contact quality of MoS_2 homojunction solar cells.

V. IMPROVEMENT OF SCHOTTKY CONTACTS

From our results it becomes apparent that developing ohmic contacts to *n* and *p* doped MoS_2 is of paramount importance to boost the efficiency of MoS_2 homojuntions. Setting aside the effect of Fremi level pinning at the MoS_2 surface, it is predicted that a low work function metal will be the best choice for *n*-MoS_2 whereas a large work function one will be suitable for *p*-MoS_2. The aligment of the work functions of several common metals to the MoS_2 energy bands is represented in Fig. 8

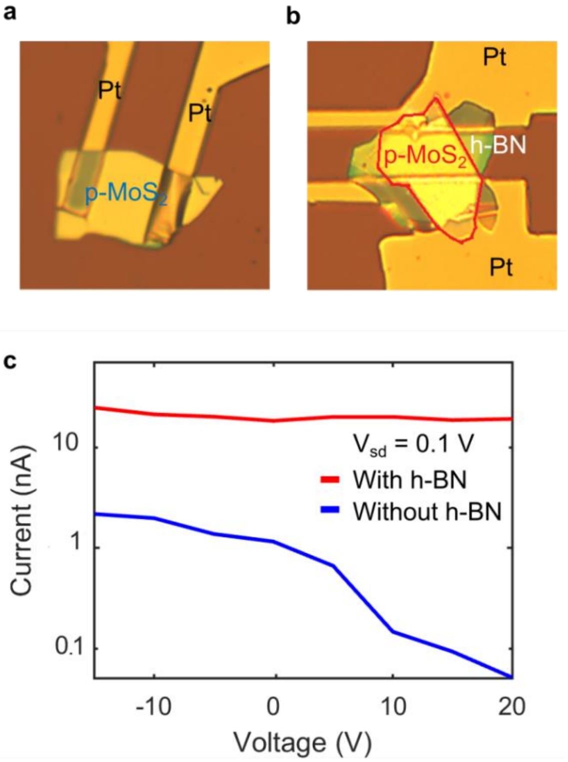

Fig 7. (a) Device consisting of *p*-MoS_2 on Pt contacts. (b) Device consisting of *p*-MoS_2 on Pt contacts with a BN buffer layer. (c) Current-V_G curve for *p*-MoS_2 without (blue curve) and with h-BN insulant layer (red curve) for a source-drain voltage of 0.1 V

In this work we have explored the evaporation of Cr/Au as n-contact. For the p side, we have tested the evaporation of Ni/Au and the use of pre-patterned Pt contacts. In all cases we have included an h-BN buffer. The results can be seen in Fig. 9. The illumination source is a halogen lamp with irradiance $2W/cm^2$. In the case of the Cr/n-Schottky contact the result is excellent (Fig. 9a). The contact is ohmic and the device has a very low resistance. It represents a great improvement with respect our original Ni contact shown in Fig. 5.

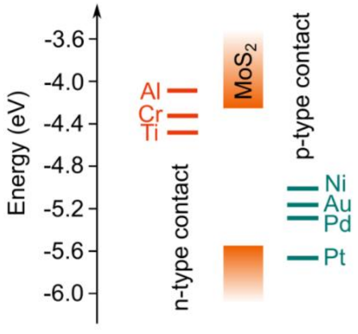

Fig 8. Band aligment of bulk MoS_2 with the work function of several common metals.

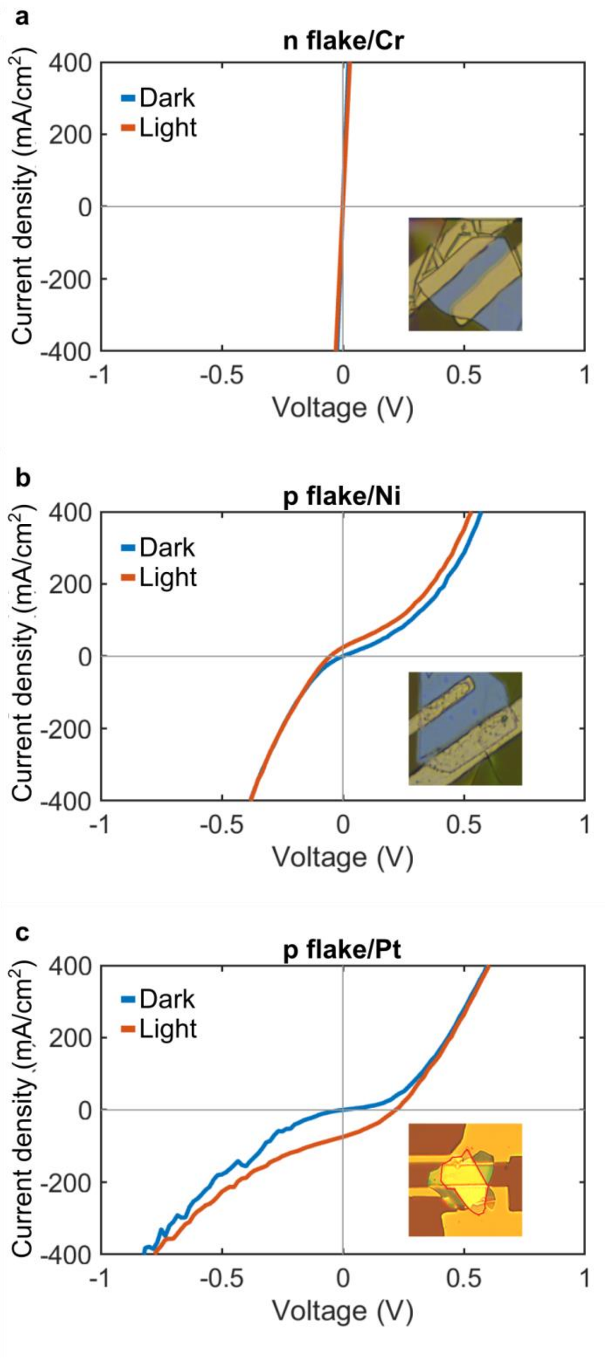

Fig 9. (a) *J-V* curves of *n*-MoS_2 with Cr/Au cotnacts.(b) *J-V* curves of *p*-MoS_2 with Ni/Au contacts. (c) *J-V* curves of *p*-MoS_2 on Pt contacts and h-BN buffer layer. Insets: Device photographs.

In the case of p-MoS_2, neither of the tested metals has provided a satisfactory result. The samples made with Ni (Fig. 9b) and Pt (Fig 9c) are clearly rectifying. They improve over the device made with Pd that was shown in Fig. 6, but much of that improvement may come from the insertion of an h-BN flake to avoid the depletion of the p-flake. More work is needed to understand why Pt does not produce better contacts to p-MoS_2 than the other metals, contradicting what is expected from the band alignment illustrated in Fig. 8.

VI. CONCLUSIONS

We have demonstrated that high V_{OC} can be reached in van der Waals TMDC solar cells by using substitutionally doped material (MoS_2 homojunctions) and by overcoming the limitations related to the metal-semiconductor contacts. An equivalent circuit model can fit the experimental results to reproduce the effect of photoactive Schottky diodes on TMDC solar cells. We have tested different metals to produce ohmic contacts onto doped MoS_2. For the *n*-doped material, the evaporation of Cr/Au generates an ohmic, low resistance contact. However, for the p-doped material, neither of the large work function metals tested (Ni, Pd, Pt) has resulted in an ohmic contact. Our results endorse the MoS_2 homojunction as a promising candidate for the development of ultra-thin photovoltaic devices and highlight the need to find ohmic contacts to *p*-MoS_2 to fully realize that potential.

REFERENCES

[1] Lee, C.-H., Lee, G.-H., van der Zande, A. M., Chen, W., Li, Y., Han, M., Cui, X., Arefe, G., Nuckolls, C., Heinz, T.F., Guo, J., Hone, J., and Kim, P. (2014). Atomically thin p–n junctions with van der Waals heterointerfaces. Nature Nanotechnology, 9(9), 676–681.

[2] Wong, J., Jariwala, D., Tagliabue, G., Tat, K., Davoyan, A. R., Sherrott, M. C., & Atwater, H. A. (2017). High Photovoltaic Quantum Efficiency in Ultrathin van der Waals Heterostructures. ACS Nano, 11(7), 7230–7240.

[3] Furchi, M. M., Höller, F., Dobusch, L., Polyushkin, D. K., Schuler, S., & Mueller, T. (2018). Device physics of van der Waals heterojunction solar cells. Npj 2D Materials and Applications, 2(1). doi:10.1038/s41699-018-0049-3.

[4] Gusakova, Julia & Wang, Xingli & Shiau, Li & Krivosheeva, A. & Shaposhnikov, Victor & Borisenko, Victor & Gusakov, Vasilii & Tay, B.K.. (2017). Electronic Properties of Bulk and Monolayer TMDs: Theoretical Study Within DFT Framework (GVJ-2e Method). physica status solidi (a). 214. 1700218. 10.1002/pssa.201700218.

[5] Suh, J., Park, T.-E., Lin, D.-Y., Fu, D., Park, J., Jung, H. J., Chen, Y., Ko, C., Jang, C., Sun, Y., Sinclair, R., Chang, J., Tongay, S. and Wu, J. (2014). Doping against the Native Propensity of MoS2: Degenerate Hole Doping by Cation Substitution. Nano Letters, 14(12), 6976–6982.

[6] Svatek, S. A., Antolin, E., Lin, D.-Y., Frisenda, R., Reuter, C., Molina-Mendoza, A. J., Muñoz, M., Agraït, Ko, T., Perez de Lara, D., N. and Castellanos-Gomez, A. (2017). Gate tunable photovoltaic effect in MoS2 vertical p–n homostructures. Journal of Materials Chemistry C, 5(4), 854–861.

[7] "Enhanced photovoltage in transition metal dichalcogenide solar cells", Simon A. Svatek, Carlos Bueno-Blanco, Der-Yuh Lin et al., to be published.

[8] Pizzocchero, F., Gammelgaard, L., Jessen, B. et al. The hot pick-up technique for batch assembly of van der Waals heterostructures. Nat Commun 7, 11894 (2016). https://doi.org/10.1038/ncomms11894

[9] Allain, A., Kang, J., Banerjee, K., & Kis, A. (2015). Electrical contacts to two-dimensional semiconductors. Nature Materials, 14(12), 1195–1205.

[10] Dun Mao, Thomas Kananen, Tiantian Li, Anishkumar Soman, Jeffrey Sinsky, Nicholas Petrone, James Hone, Po Dong, and Tingyi Gu. Bandwidth Limitation of Directly Contacted Graphene–Silicon Optoelectronics. ACS Applied Electronic Materials 2019 1 (2), 172-178.

[11] Liu, Y., Guo, J., Zhu, E. et al. Approaching the Schottky–Mott limit in van der Waals metal–semiconductor junctions. Nature 557, 696–700 (2018).

[12] Kim, C., Moon, I., Lee, D., Choi, M. S., Ahmed, F., Nam, S., Cho, Y., Shin, H., Park, S. and Yoo, W. J. (2017). Fermi Level Pinning at Electrical Metal Contacts of Monolayer Molybdenum Dichalcogenides. ACS Nano, 11(2), 1588–1596.

[13] Cui, X., Lee, G., Kim, Y. et al. Multi-terminal transport measurements of MoS2 using a van der Waals heterostructure device platform. Nature Nanotech 10, 534–540 (2015). https://doi.org/10.1038/nnano.2015.70